Poly(N-Isopropylacrylamide) Microparticles Produced by Radiation Pressure of a Focused Laser Beam: A Structural Analysis by Confocal Raman Microspectroscopy Combined with a Laser-Trapping Technique

Yasuyuki Tsuboi,*,†,‡ Masayuki Nishino,† Tetsuya Sasaki,† and Noboru Kitamura*,†

Division of Chemistry, Graduate School of Science, Hokkaido University, Sapporo 060-0810, Japan, and SORST (Solution Oriented Research for Science and Technology), JST (Japan Science and Technology Corporation), Japan

Received: November 8, 2004; In Final Form: February 7, 2005

We developed a confocal Raman microspectroscopy system combined with a laser trapping technique and applied it to aqueous solutions (H_2O and D_2O) of poly(N-isopropylacrylamide) (PNIPA), which is well-known as a representative thermo-responsive polymer, i.e., phase transition/separation between coiled and globular states. By introducing a near-infrared (1064 nm) laser beam into a microscope, PNIPA microparticles were produced at the focused spot of the laser beam, both in H_2O and D_2O. By using the present system, we succeeded in obtaining the Raman spectra of PNIPA in the coiled and globular states over a wide wavenumber region (800−3500 cm^{-1}) for the first time. For the D_2O solutions (in which the photothermal effect is negligible and hence the microparticles should be produced purely by the effect of radiation pressure), some significant differences were observed in the Raman spectra for the coiled state, in the globular state, and for laser induced microparticles. By analyzing these spectra in detail, we revealed that the structure of the laser-induced microparticles was analogous to that in the globular state. We also discuss the fundamental mechanism underlying the transformation of the higher order structure of a polymer by radiation pressure.

Introduction

Conformational/higher-order structural changes of polymers have attracted much attention in various research fields. For instance, proteins in solution phase adopt optimized higher-order structures, represented by a coil, an α-helix, or a β-sheet phase, in accordance with external stimuli, as well as changes caused by surrounding environmental factors such as temperature, pressure and pH: so-called "folding". Several artificial polymers in solution phase also exhibit analogous structural changes with high sensitivity, and these are quite important as a model of the natural systems mentioned above. A representative example of such a polymer is poly(N-isopropylacrylamide), abbreviated as PNIPA, whose folding phenomenon has a long research history.[1] In aqueous solution at room temperature, PNIPA is homogeneously dissolved and adopts a coiled structure, while it shows a lower critical solution temperature (LCST) at around 305 K. Above this temperature the solution exhibits a coil−globule transition, resulting in a macroscopic phase separation due to the aggregation of globules. The coil−globule transition of an aqueous PNIPA solution is related to hydrophobic interactions between the polymer backbones and hydration of the amide groups in PNIPA. Since PNIPA is a promising prototype for understanding the fundamental mechanisms underlying the issue of polymer folding and related structural changes, the coil−globule transition of PNIPA has been investigated by various methods: light-scattering,[1−5] calorimetry,[6,7] NMR,[8] and fluorescence spectroscopy.[9,10]

On the other hand, analogous phenomena to those mentioned above can be induced for an aqueous PNIPA solution, not only by a temperature change, but also by laser irradiation.[11] In 1993, Ishikawa et al. demonstrated that the formation/ disappearance of a single PNIPA microparticle could be controlled by switching on/off of a focused infrared laser beam (1064 nm) under an optical microscope.[12] Their results were explained by local heating of the PNIPA solution by absorption of the incident laser beam by H_2O through the overtone O−H stretching band at 1064 nm. Following this work, Hofkens et al. reported that laser-induced PNIPA particle formation could be observed even in heavy water.[13] Since D_2O is transparent at 1064 nm, PNIPA particle formation could not be explained by photothermal effects, unlike the case of particle formation in H_2O. Furthermore, on the basis of simultaneous observations of laser-induced particle formation and fluorescence microspectroscopy of an aqueous pyrene-labeled PNIPA solution,[14] they reported that the formation/disappearance behavior of the polymer particles was different between H_2O and D_2O, and they concluded that particle formation in the case of D_2O was due to radiation pressure, whereby the PNIPA polymer chains were aggregated, resulting in the formation of microparticles.[13−15] It is also noteworthy here that Juodkazis and Misawa et al. have demonstrated radiation pressure can induce reversible-shrinkage of a micro-rod of PNIPA gel.[16] Relevant to above, Masuo et al. observed contraction and swelling of a molecular assembly of a dendrimer in response to the switching on-and-off of a near-infrared laser beam: i.e., radiation pressure.[17] Thus, the interaction of radiation pressure with polymeric materials is of great interest.

The formation of laser-induced PNIPA microparticles in D_2O demonstrates that radiation pressure can act as a manipulative force at the molecular level, as predicted by the Rayleigh

* Corresponding authors. E-mail: twoboys@sci.hokudai.ac.jp (YT), kitamura@sci.hokudai.ac.jp (NM).

† Hokkaido University.

‡ JST.

10.1021/jp044894b CCC: $30.25
Published on Web 03/17/2005

scattering theory.[18] Besides the above examples, interactions between radiation pressure generated by a focused laser beam and nano/micro materials have been reported in practical applications: micells,[19] vesicules,[20] synthetic polymers beads,[21] and so forth.[22,23] Although the main issues of these studies are laser trapping[24,25] and/or laser control of the morphology of the material, the PNIPA system mentioned above is quite unique, since radiation pressure exerted on the nanometer-sized polymer chains produces micrometer-sized particles, and these particles are laser-trapped simultaneously. To understand how radiation pressure influences the conformation of a PNIPA chain, the structures of the laser-induced PNIPA microparticles should be elucidated experimentally. Nonetheless, the detailed structures of the particles still remain unclear. We consider that one possible approach along the lines mentioned above is the application of Raman spectroscopy to the PNIPA system, since it is widely known that this technique is very sensitive to molecular structures and can be readily extended to experiments under an optical microscope in noncontact mode.[21,22]

So far, a number of research groups have reported the infrared (IR) absorption spectra of an aqueous PNIPA solution[26−29] before and after the phase transition along with theoretical calculations[28] of the spectra of the related systems. By contrast, Raman spectroscopy of PNIPA solution systems has hitherto been limited to few studies. In 1993, Terada et al. reported Raman spectral changes of water molecules during the phase transition of PNIPA in H_2O.[30] Very recently, Maeda et al. reported confocal Raman microspectroscopy of aqueous PNIPA solutions at a very high concentration (50 wt %).[31] In addition to studies of these aqueous PNIPA solutions, several research groups have also shown Raman spectra of PNIPA gels (i.e., cross-linked PNIPA).[32,33] It is worth noting that the Raman spectra reported are limited to the wavenumber (ν) region of 2500−4000 cm^{-1}. In this region, only an intense Raman band due to the C−H stretching mode of the methylene group (main chain) in PNIPA is observed at around 2960 cm^{-1} in addition to a band due to H_2O (O−H stretching at around 3400 cm^{-1}). However, the Raman signals due to the skeletal vibrations of PNIPA are very weak, and to the best of our knowledge, the Raman spectrum of an aqueous PNIPA solution below 2500 cm^{-1} has never been reported, except for those of PNIPA gels.[34] For PNIPA gels, Appel et al. have revealed the Raman spectrum in the 800−1800 cm^{-1} region (where the skeletal vibrations are seen), while Suzuki et al. have reported the spectra in the much lower wavenumber region of $\nu < 250$ cm^{-1}, where the bending/stretching modes of water molecules involved in the gels are detected.[35] Thus, to obtain insights into the structure of laser-induced PNIPA particles, it is indispensable to study the Raman signals of the skeletal vibrations of the polymer at $\nu < 2500$ cm^{-1}.

In the present study, we succeeded in observing the Raman spectra of an aqueous PNIPA solution and of laser-induced PNIPA particles over a wide wavenumber region (800−3000 cm^{-1}), which can provide invaluable information about the polymer structures. On the basis of the Raman spectra, we demonstrate that radiation pressure can induce both the coil−globule structural change and the molecular assembly of PNIPA.

Experimental Section

Chemicals and Sample Preparation. The same poly(N-isopropylacryleamide) (MW = 5.2×10^5) sample was used as reported previously.[36] The present PNIPA in water exhibited LCST at 305 K, which agreed very well with the literature value.[1] The polymer was dissolved in distilled/ deionized water (Advantec, GSR-200) or heavy water (Aldrich, 99.999% or Wako, 99.9%; both gave the same results). The concentrations of the sample solutions were fixed at 4.0 wt % throughout the study. For the experiments using D_2O, the samples were kept in a desiccator during the dissolution process until they were used for measurements, and fresh samples were always used to avoid contamination with H_2O from the air. The sample solutions were placed between two glass plates (Matsunami glass, thickness: 0.15 and 0.8 mm), which were rinsed with D_2O before use, and edges of the plates were sealed with a paste. These sample cells were used for the subsequent measurements. The thickness of the liquid membrane in the cell was c.a. 100 μm.

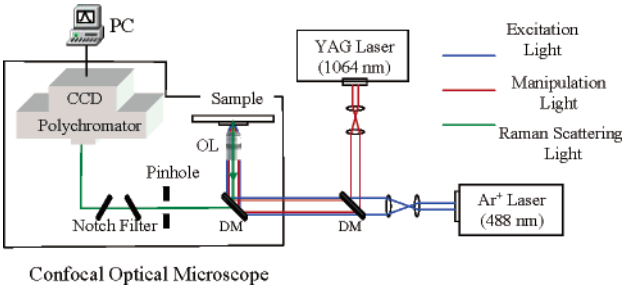

Figure 1. Experimental setup of the present confocal Raman microspectroscopy system combined with a laser trapping technique. DM, dichroic mirror; OL, objective lens. A YAG laser (1064 nm) and an Ar laser (488 nm) were used for laser-trapping and for excitation for Raman scattering, respectively. The two notch filters were utilized to eliminate Rayleigh scattering light from the two lasers (488 and 1064 nm). The pinhole was inserted to achieve a confocal arrangement.

Confocal Raman Microspectroscopy. Figure 1 shows the optical setup of the present confocal Raman microspectroscopy system. A CW Nd^{3+}: YAG laser ($\lambda = 1064$ nm, Spectron Laser Systems, SL-902T) was used to generate radiation pressure, while an Ar^+ laser beam ($\lambda = 488$ nm, Coherent, Innova 70) was used as the excitation light source for Raman scattering. The two laser beams were introduced coaxially into an inverted optical microscope (Nikon, ECLIPSE E300) by using a dichroic Mirror (DM) and were irradiated to a sample solution through an oil-immersion objective lens (×100, NA = 1.30). Raman-scattering light was passed through a pinhole with a diameter of 100 μm to ensure the confocal arrangement, and incident light and Rayleigh scattering light were removed by passing through two holographic notch filters for 488 and 1064 nm laser light (Kaiser Optics). Raman-scattering light was then detected with a cooled CCD camera (220 K, Andor Tec.) equipped with a polychromator (grating; 1200 grooves/mm). The spatial resolution along the lateral and vertical directions were 0.25 and 2.4 μm, respectively, and the spectral resolution was 2.0 cm^{-1}. The effective laser power irradiated to the sample solution on the microscope stage (P_{in}; laser power after passing through the objective lens) was evaluated by the method reported by Misawa et al.[37] The ratio of P_{in} to the incident laser power before introducing it to the microscope (P_{out}) was $P_{in}/P_{out} = 0.11$ in the present system.

Results and Discussion

Raman Spectra of PNIPA in the Coiled and Globular States. To discuss the Raman spectra characteristics of the laser-induced (radiation pressure induced) PNIPA microparticles (and thus the structure of the particles), we need to reveal the Raman spectra of PNIPA in the coiled (below LCST) and globular states (above LCST).Therefore, we measured the Raman spectra of PNIPA in H_2O and D_2O (4.0 wt %) without 1064 nm laser

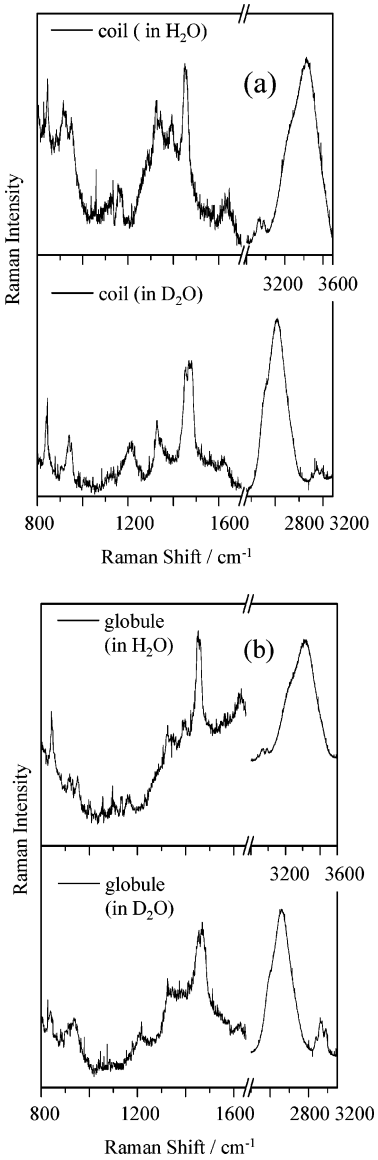

Figure 2. Reference Raman spectra of PNIPA obtained in the absence of YAG laser irradiation. (a) Raman spectra of the coiled state of PNIPA measured for dilute solutions (4.0 wt %) of H_2O (upper panel) and D_2O (lower panel). Temperature of the sample was 293 K. (b) Raman spectra of the globular states of PNIPA measured for dilute solutions (4.0 wt %) of H_2O (upper panel) and D_2O (lower panel). Temperature of the sample was 305 K.

irradiation by using the present confocal Raman microspectroscopy system. In the experiments, we employed a thermostatic microscope stage to control the temperature of the PNIPA sample solutions, both below and above LCST. The Raman spectra of PNIPA that were obtained in H_2O and D_2O (both 4.0 wt %) in the coiled (a) and globular states (b) are shown in Figure 2. It is worth emphasizing that Raman spectra over a wide wavenumber region (800−3500 cm^{-1}) can be obtained with good signal-to-noise ratios on the basis of the confocal arrangement (diameter of pinhole = 100 μm), while a very broad spectrum was obtained without the pinhole. The spectra shown in Figure 2 roughly agree with the spectrum of a relevant cross-linked polymer material (a macro porous PNIPA gel) with respect to their peak position.[34] The spectra in Figure 2 are the first demonstration of the Raman spectra of the PNIPA backbone in aqueous solutions.

On the basis of the spectra with high S/N ratios, we assigned the main vibrational peaks by reference to the relevant IR spectra

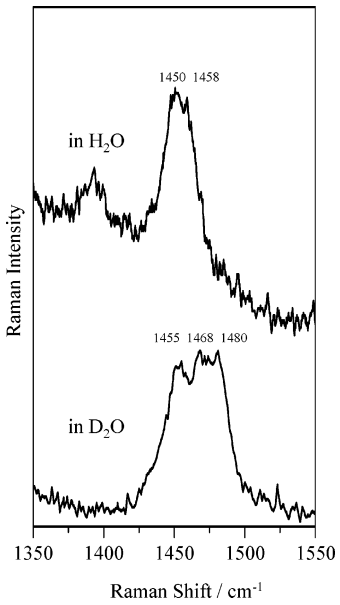

Figure 3. Expanded Raman spectra of the coiled states in H_2O (upper spectrum) and D_2O (lower spectrum). The band at 1450 cm^{-1} is attributable to the CH_3 symmetric deformation mode, while the peak at 1480 cm^{-1} in D_2O is ascribed to the amide II band.

and theoretical calculations, the results of which are summarized in Tables 1 and 2. The amide group in PNIPA should exhibit the characteristic amide I and II bands. In practice, PNIPA shows the amide I and II bands at around 1620−1650 and 1560 cm^{-1}, respectively, in the IR spectrum. However, these bands are very weak and ambiguous in the Raman spectra due to the selection rules. Instead of the amide bands, various Raman peaks characteristic of the present system were observed.

A close inspection of Tables I and II and Figure 2 reveals various differences in the spectra between H_2O and D_2O. In particular, the difference in the CH_3 antisymmetric deformation (or CH_2 bending/CH deformation) band at around 1450 cm^{-1} is worth noting. To discuss the point more clearly, the expanded spectra of PNIPA in the coiled state in H_2O and D_2O are shown in Figure 3. The spectrum in H_2O exhibited two peaks at 1450 and 1458 cm^{-1}, while that in D_2O was split into complicated peaks with slightly higher wavenumber shifts (1455 and 1468 cm^{-1}). Such peak-splitting of the CH_3 antisymmetric deformation band in H_2O and D_2O have also been reported for the relevant IR absorption spectra.[28,29] However, the intensity ratio of the lower and higher wavenumber peaks (I_{1450}/I_{1458}) in H_2O was reversed from that in D_2O (I_{1455}/I_{1468}). Furthermore, an additional peak was observed at 1480 cm^{-1} in D_2O. According to the literature, the hydrogen atom of the amide group (H−N) can be readily replaced by deuterium in D_2O,[28,29] such that it gives rise to a shift to lower frequency of the amide II band, from 1560 to 1480 cm^{-1}. Therefore, the weak peak observed in D_2O is ascribed to the amide II band, involving coupling of the N−H bending and C−N stretching modes.

Another characteristic of the Raman spectrum in D_2O was also confirmed. Although Maeda et al. reported that the IR bands of the main chain and the isopropyl groups in PNIPA were essentially the same for both H_2O and D_2O,[29] the present Raman spectroscopy revealed that the peaks responsible for the C−C skeletal vibration in the lower frequency region of <1000 cm^{-1} observed in H_2O were different from those in D_2O, and the peak ascribed to the CH_3 symmetric deformation observed in H_2O at 1390 cm^{-1} disappeared in D_2O. It is noteworthy here that analogous behavior is observed in the globular state (see Tables and Figure 2b). These results strongly suggest the presence of

TABLE 1: Observed Raman Frequencies and Assignments of the Individual Bands Observed for the Laser-Induced Particles and the Coiled and Globular States in H_2O Solution

wavenumber (cm^{-1})				
laser-induced particle	coiled state	globular state	assignments	ref.
845, 920, 948	842, 919, 951	845, 920, 950	CC skeletal vibration	34
1130	1131	1133	CH_3 rocking	28
1156	1158	1155	amide III	28
1321	1325	1323, 1343	CH deformation	34
1393	1397	1393	CH_3 symmetric deformation	28
			CH_3 antisymmetric deformation	29
1452	1450, 1458	1452	CH_3 symmetric deformation	28
			CH_2 bending	34
			CH deformation	29
1560	1560	1560	amide II	28, 29, 34
1635	1630	1635	amide I	28, 34
2878	2878	2878	symmetric CH stretching CH_3	29, 31
2924	2924	2924	antisymmetric CH stretching of CH_2	29, 31
2943	2943	2938	antisymmetric CH stretching of CH_2	29, 31
2980	2983	2977	antisymmetric CH stretching of CH_3	29, 31

TABLE 2: Observed Raman Frequencies and Assignments of the Individual Bands Observed for the Laser-Induced Particles and the Coiled and Globular States in D_2O Solution

wavenumber (cm^{-1})				
laser-induced particle	coiled state	globular state	assignments	ref.
838, 939	838, 939	838, 937	CC skeletal vibration	34
1133	1133		CH_3 rocking/skeletal vibration of CH_3	28, 29
1325	1325	1325	CH deformation	34
1455	1455, 1468	1455	CH_3 symmetric deformation	28
			CH_2 bending	34
			CH deformation	29
1470	1468, 1480	1470	amide II	29
1623	1616	1626	amide I	29
2880	2880	2880	symmetric CH stretching of CH_3	29, 31
2922	2922	2922	antisymmetric CH stretching of CH_2	29, 31
2945	2945	2945	antisymmetric CH stretching of CH_2	29, 31
2978	2983	2978	antisymmetric CH stretching of CH_3	29, 31

complicated coupling interactions among these vibrations through the polymer chain. These characteristics of the Raman spectra should be compared with those of the laser-induced PNIPA particles produced in H_2O and D_2O.

Raman Spectra of Laser-Induced PNIPA Particles in H_2O and D_2O Solutions. We confirmed the 1064 nm laser-induced formation of PNIPA particles in H_2O, as reported previously by Ishikawa et al.[12,15] and Hofkens et al.[13] Figure 4 displays typical optical micrographs of the particles produced at several laser powers (P_{in}). A single PNIPA particle was produced immediately after 1064 nm laser irradiation (<0.1 s) and, after irradiation for several tens of seconds (>30 s), the size of the particle reached an equilibrium value, depending on the incident laser beam intensity: P_{in}. The photographs shown in Figure 4 were taken at the equilibrium state at a given P_{in}. The PNIPA particle was simultaneously laser-trapped with the formation of the particle at the focal spot of the laser beam. After switching off the laser beam, the particle disappeared immediately (<0.1 s). As described in the preceding section, particle formation is ascribed to local heating of the solution phase at the focused spot of the laser beam through absorption of H_2O at 1064 nm.

On the other hand, the formation and dispersal processes of the laser-induced PNIPA particles in D_2O were obviously different from those in H_2O, as reported by Hofkens et al.[13] For example, it took several minutes of laser irradiation to grow a particle large enough to be observable under the microscope, and the maximum size of the particle was less than 3 μm, even at $P_{in} = 0.26$ W. This is close to the size described in a previous work (3−4 μm).[13] In addition, the size of the particle in the equilibrium state was almost the same however long it was observed under the microscope, irrespective of P_{in}, as shown in Figure 5a. Furthermore, the particle disappeared very slowly after switching off the laser; it took several tens of seconds to dissolve the particle completely in D_2O. In D_2O, the photothermal effect is negligible, and hence the origin of particle formation is ascribable to radiation pressure.[13,14]

Since the formation processes of PNIPA microparticles by laser irradiation are different between H_2O and D_2O, as described above, the structures of the particles produced in each medium should be different from each other. Therefore, we measured the Raman spectra of the particles shown in Figures 4b and 5b for the H_2O and the D_2O samples, respectively. The Raman spectra of the laser-induced PNIPA particles in H_2O and D_2O were similar to those observed for the polymer in the coiled and/or globular states shown in Figure 2. However, the Raman shift of each vibrational band observed for the laser-induced particles formed in D_2O was different from those formed in H_2O and the coiled states in H_2O and D_2O. In the following section, we discuss the detailed results of the Raman spectra.

Raman Spectra of PNIPA in the Coiled/Globular States, and Laser-Induced Particles in D_2O. To reveal the structures of the PNIPA particles produced by radiation pressure in D_2O, we carefully compared the Raman spectrum of these particles with those of PNIPA in the coiled and globular states. Figure 6 shows the expanded Raman spectra of the species for the frequency regions of interest.

In the wavenumber region between 1000 and 1400 cm^{-1} (Figure 6a), the PNIPA sample in the coiled state (top spectrum) in D_2O showed the O−D bending signal of the solvent itself at 1210 cm^{-1} in addition to the peak due to the CH deformation mode of PNIPA (1325 cm^{-1}). This is very reasonable, since

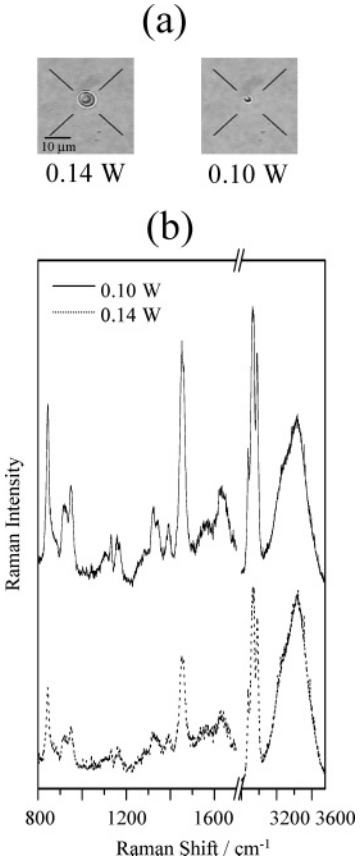

Figure 4. Optical micrographs of laser-induced microparticles in H_2O (a) and their Raman spectra (b). The incident power of the YAG laser (P_{in}) is given in the figure.

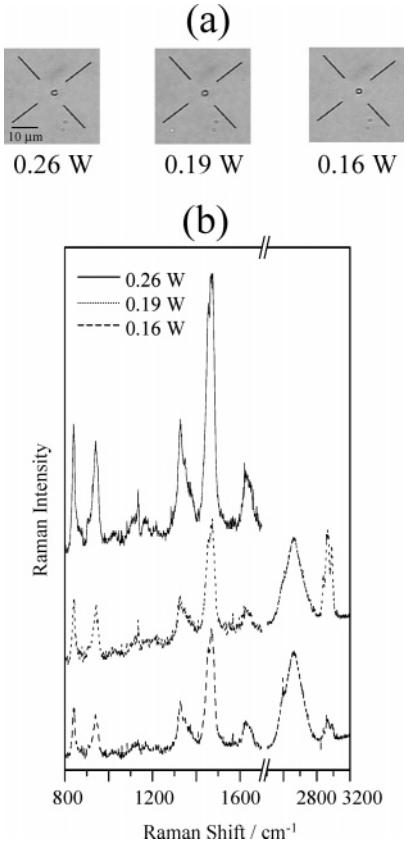

Figure 5. Optical micrographs of laser-induced microparticles in D_2O (a) and their Raman spectra (b). The incident power of the YAG laser (P_{in}) is given in the figure.

the polymer in the coiled state is dissolved homogeneously in D_2O. By contrast, the O−D bending band disappeared for the laser-induced PNIPA particle (bottom spectrum). This indicates that D_2O molecules are excluded from the particle; this will be discussed again later.

The spectra in the frequency region between 1350 and 1550 cm^{-1} are also shown in Figure 6b. The polymer in the coiled state (top spectrum) exhibited three vibrational peaks. As described previously, the band at 1480 cm^{-1} is ascribed to the amide II band, which is shifted to lower frequency in D_2O compared to in H_2O, while the bands responsible for the CH_3 deformation mode/CH_2 bending and amide II are superimposed at 1450 and 1470 cm^{-1}. In comparison with the spectrum in the coiled state, the intensity of the amide II band (1480 cm^{-1}) is rather weak, and the peak almost disappears in the globular state (middle spectrum). The spectral changes are very characteristic to the coil−globule transition of PNIPA. This is supported by the fact that analogous spectral changes (i.e., reduction of the amide II band intensity in the globules) to those observed in the present study were suggested in the infrared absorption spectrum during the phase transition of PNIPA in D_2O.[29] Furthermore, for the Raman spectrum of the PNIPA particles produced by the radiation pressure (bottom spectrum), it is worth emphasizing that the amide II band almost disappears and the spectrum is clearly analogous to that of PNIPA in the globular state, demonstrating that laser-induced PNIPA particles are made up of chains of globules.

At >2000 cm^{-1} (Figure 6c), on the other hand, the spectrum is characterized by the C−H stretching vibrations of the main chain PNIPA, showing peaks in the frequency region between 2750 and 3100 cm^{-1}. The C−H stretching vibrational bands in the globular state and the laser-induced particles were observed as broad peaks, while that of the coiled state split into peaks at 2945 and 2922 cm^{-1}. Furthermore, the peak at 2945 cm^{-1} in the coiled state was somewhat more intense than that at 2922 cm^{-1}. By contrast, the relative peak intensity was reversed in the spectrum of the globular state (middle spectrum). Very recently, Maeda et al. reported an analogous Raman spectrum to that in Figure 6c for a concentrated aqueous solution of PNIPA (50 wt %).[31] In addition, it has been reported that the C−H stretching band exhibits a slight high-frequency shift by hydration of the C−H group.[38] Therefore, the change in the relative intensity upon the phase transition (from coil to globule) is ascribed to the dehydration of the methylene chain of PNIPA in the globular state. An analogous spectral change was clearly observed for the laser-induced PNIPA particles, and the spectral shape was similar to that of the globules. On the other hand, Figure 6d displays the spectra of the O−D stretching bands of the solvent at around 2500 cm^{-1}, whose intensity is normalized to that at the C−H stretching band. In a similar way to Figure 6a, a decrease in intensity of the O−D vibrational band was also observed for the laser-induced particles, demonstrating that D_2O molecules were excluded from the particles produced at the focus spot of the incident laser beam.

In H_2O, analogous results to those mentioned above were observed (irrespective of the laser power) for the laser-induced particles. Changes in the relative intensity of the two peaks of the CH_2 stretching band at around 2930 cm^{-1} were also observed upon the phase transition in H_2O. However, hardly any significant spectral differences were observed between the three species (coil, globule, and laser-induced particles) in the other frequency regions.

The dehydration of the polymer chains has been thus indicated for the laser-induced microparticles both in D_2O and H_2O. The

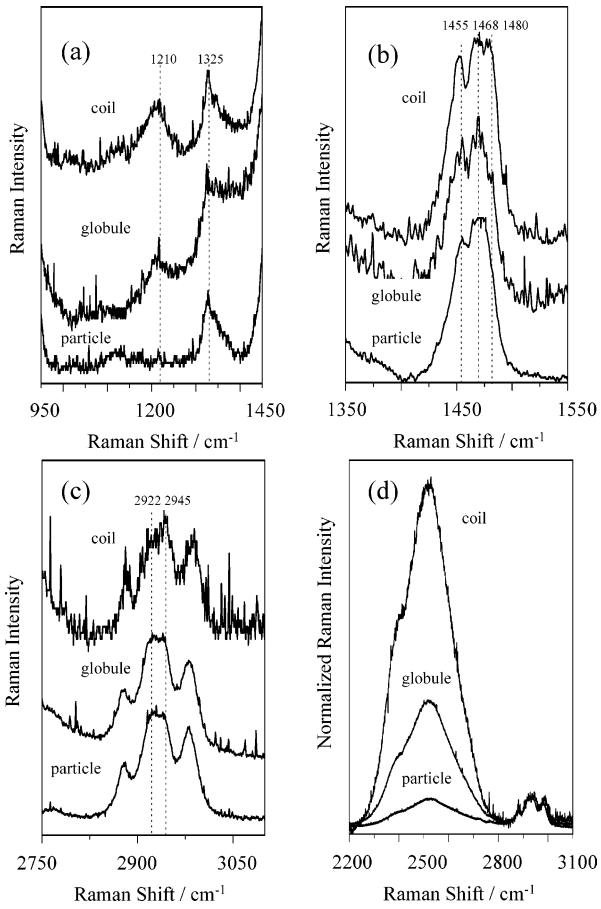

Figure 6. Raman spectra of the laser-induced particle (top spectra in each pannel, $P_{in} = 0.19$ W), the globular state (middle spectra in each pannel), and the coiled state (bottom spectra in each pannel) in D_2O. (a) Expanded spectra around 1000−1400 cm^{-1}. The band at 1325 cm^{-1} is ascribed to the CH_3 antisymmetric deformation mode, while the band at 1210 cm^{-1} is ascribed to the O−D stretching vibration of the solvent (D_2O). (b) Expanded spectra around 1350−1550 cm^{-1}. The band at 1450 cm^{-1} is ascribed to the CH_3 symmetric deformation mode, while the peak at 1480 cm^{-1} is ascribed to the amide II band. (c) Expanded spectra around 2750−3100 cm^{-1}. The observed peaks are ascribed to the C−H stretching vibration. Peak-splitting was observed at the center band into 2925 and 2945 cm^{-1}. The relative intensity of the two peaks reflects the degree of hydration/dehydration (see text). (d) Expanded spectra of the O−D stretching bands around 2500 cm^{-1}. The spectra were normalized to the intensity at the C−H stretching band at 2940 cm^{-1}.

phase transitions from the coiled state to the globular state were induced by the radiation pressure and the local heating in D_2O and H_2O, respectively. As previously mentioned, while the particles in H_2O disappeared rapidly after switching off the laser beam, it took several tens of minutes in D_2O. This strongly implies a structural difference between the particle in D_2O and that in H_2O. The Raman spectrum of the particle in D_2O indicated the exclusion of the solvent molecules (D_2O) from the particle. This means an increase in the concentration of PNIPA at the focal point. On the basis of these results, we may conclude that the density of the polymer chain in the particle in D_2O is higher than that in H_2O. Consequently, the conformation of the polymer chain in the particle in D_2O would take a more compact structure as compared to that in H_2O.

Formation Mechanism of the Laser-Induced Particles in D_2O. The refractive index of PNIPA ($n = 1.508$)[13] is higher than that of heavy water ($n = 1.338$), and the hydrodynamic radius of PNIPA used in the present study (M.W. $= 5.2 \times 10^5$) is estimated to be 50−100 nm (globule−coil).[13] Under such condition, the radiation pressure overcomes the Brownian motion of the polymer in water, as Hofkens et al. suggested.[13] In more detail, the origin of the radiation pressure in the present study is the dipole gradient force. The free energy of the system becomes lower when the more polarizable (i.e., higher refractive index) molecules replace D_2O at the focal point.[39] Such a effect can induce the assembling of molecules, the conformational changes, and the deformation of molecular assemblies.[40]

The Raman spectrum of the laser-induced particles in D_2O was shown to be analogous to that of PNIPA in the globular state, demonstrating that the laser-induced particles consisted of the globular polymer chains. Furthermore, a large proportion of D_2O molecules was shown to be excluded from the particles produced in the focused area of a 1064-nm-laser beam. On the basis of these results, laser-induced PNIPA particle formation in D_2O can be explained as follows. First, PNIPA molecules possessing coiled structures that are dissolved homogeneously in D_2O are attracted toward the focused spot of the incident laser beam through radiation pressure exerted on the molecules. With the increase in the local concentration of the PNIPA molecules at the focal spot, a stronger radiation pressure will be exerted on the PNIPA aggregates. Since the density of the PNIPA molecules at the focal spot becomes higher, D_2O molecules initially hydrated to the polymer should be excluded due to an increase in hydrophobic interactions between the polymers. The radiation pressure thus promotes dehydration of the PNIPA via assemblage of the polymer molecules, which implies the transition of PNIPA from the coiled state to a globular structure. This is what is actually observed in the present study.

Conclusions

To analyze the PNIPA microparticles formed by radiation pressure of a focused near-infrared laser beam, we developed a system of confocal Raman microspectroscopy combined with a laser trapping technique. The Raman spectra of PNIPA in its coiled and globular states in dilute aqueous solutions (H_2O and D_2O) were measured for the first time. Significant differences were observed between the spectra of H_2O and D_2O samples, not only for the amide band but also for the bands responsible for the skeletal vibration of PNIPA. This implies the participation of complicated vibrational coupling interactions through the polymer chains. In the cases of the spectra of PNIPA in the coiled and globular states and for laser-induced particles, we observed hardly any significant differences in the H_2O samples. However, we confirmed apparent spectral differences in the amide II band and the C−H stretching band for samples in D_2O. The Raman spectrum of the laser-induced particles was ascribable to their being in the globular state. Furthermore, the exclusion of D_2O molecules from the particles was clearly observed. Radiation pressure can cause the PNIPA molecules to aggregate with the exclusion of D_2O molecules, i.e., dehydration, promoting the coil−globule transition. The present study clearly demonstrates that the radiation pressure can convert the higher-order structures of PNIPA from the coiled to globular state during particle formation.

Acknowledgment. The authors are grateful to Dr. Y. Katsumoto (Hiroshima University) and Miss. K. Tsuda (Kwansei Gakuin University) for their helpful advice. We also wish to thank Dr. J. Hotta (Hokkaido University) for valuable discussions. Y.T. acknowledges financial support from the Yamada Science Foundation. This work was partly supported by a Grant-

in-Aid from the Ministry of Education, Culture, Sports, Science and Technology of Japan to Y.T. (16750001).

References and Notes

(1) Heskins, M.; Guillet, J. E. *J. Macromol. Sci. Chem. A* **1968**, *2*, 1441.
(2) Fujishige, S.; Kubota, K.; Ando, I. *J. Phys. Chem*. **1989**, *93*, 3311.
(3) Tong, Z.; Zeng, F.; Zheng, X.; Sato, T. *Macromolecules* **1999**, *32*, 4488.
(4) Kubota, K.; Fujishige, S.; Ando, I. *Polym. J*. **1990**, *22*, 15.
(5) Wang, X.; Qiu, X.; Wu, C. *Macromolecules* **1998**, *31*, 2972.
(6) Schild, H. G.; Tirrell, D. A. *J. Phys. Chem*. **1990**, *94*, 4352.
(7) Tiktopulo, E. I.; Bychkova, V. E.; Ricka, J.; Ptitsyn, O. B. *Macromolecules* **1994**, *27*, 2879.
(8) Ohta, H.; Ando, I.; Fujishige, S.; Kubota, K. *J. Polym. Sci. B: Polym. Phys*. **1991**, *29*, 963.
(9) Winnik, F. M. *Macromolecules* **1990**, *23*, 233.
(10) Walter, R.; Ricka, J.; Quellet, C.; Nyffenegger, R.; Binkert, T. *Macromolecules* **1996**, *29*, 4019.
(11) Kitamura, N.; Ishikawa, M.; Misawa, H.; Fujisawa, R. Laser-controlled phase transition of aqueous poly(N-isopropylacrylamide) solution in micrometer domain. In *Microchemistry-Spectroscopy and Chemistry in Small Domains*; Masuhara, H., De Schryver F. C., Kitamura, N., Tamai, N., Eds.; North-Holland: Amsterdam, 1944.
(12) Ishikawa, M.; Misawa, H.; Kitamura, N.; Masuhara, H. *Chem. Lett*. **1993**, 481.
(13) Hofkens, J.; Hotta, J.: Sasaki, K.; Masuhara, H.; Iwai, K. *Langmuir* **1997**, *13*, 414.
(14) Hofkens, J.; Hotta, J.; Sasaki, K.; Masuhara, H.; Taniguchi, T.; Miyashita, T. *J. Am. Chem. Soc*. **1997**, *119*, 2741.
(15) Ishikawa, M.; Misawa, H.; Kitamura, N.; Fujisawa, R.; Masuhara, H. *Bull. Chem. Soc. Jpn*. **1996**, *69*, 59.
(16) Juodkazis, S.; Mukai, N.; Wakaki, R.; Yamaguchi, A.; Matsuo, S.; Misawa, H. *Nature* **2000**, *408*, 178.
(17) Masuo, S.; Yoshikawa, H.; Asahi, T.; Masuhara, H.; Sato, T.; Jiang, D.; Aida, T. *J. Phys. Chem. B* **2002**, *106*, 905.
(18) Shen, Y. R. *The Principles of Nonlinear Optics*; John Wiley & Sons: New York, 1984.
(19) Hotta, J.; Sasaki, K.; Masuhara, H. *J. Am. Chem. Soc*. **1996**, 118, 11968.
(20) Kitamura, N.; Sekiguchi, N.; Kim, H.-B. *J. Am. Chem. Soc*. **1998**, *120*, 1942.
(21) (a) Ajito, K.; Torimitsu, K. *Appl. Spectrosc*. **2002**, *56*, 541. (b) Crawford, K. D.; Hughes, K. D. *J. Phys. Chem. B* **1998**, *102*, 2325.
(22) (a) Houlne, M. P.; Sjostrom, C. M.; Uibel, R. H.; Kleimeyer, J. A.: Harris, J. M. *Anal. Chem*. **2002**, *74*, 4311. (b) Urlaub, E.; Lankers, M.; Hartmann, I.; Popp, J.; Trunk, M.; Kiefer, W. *Chem. Phys. Lett*. **1994**, *231*, 511.
(23) Bustamante, C.; Bryant, Z.; Smith, S. B. *Nature* **2003**, *421*, 423.
(24) Ashkin, A. *Phys. Rev. Lett*. **1970**, *24*, 156.
(25) Ashkin, A.; Dziedzic, J. Yamane, T. *Nature* **1987**, *330*, 769.
(26) Plate, N. A.; Lebedeva, T. L.; Valuev, L. I. *Polym. J*. **1999**, *31*, 21.
(27) Percot, A.; Zhu, X. X,; Lafleur, M. *J. Polym. Sci. B: Polym. Phys* **2000**, *38*, 907.
(28) (a) Katsumoto, Y.; Tanaka, T.; Sato, H.; Ozaki, Y. *J. Phys. Chem. A* **2002**, *106*, 3429. (b) Katsumoto, Y.; Tanaka, T.; Ozaki, Y. *Kobunshi Robunshu* **2003**, *60*, 256.
(29) (a) Maeda, Y.; Higuchi, T.; Ikeda, I. *Langmuir* **2000**, *16*, 7503. (b) Maeda, Y.; Nakamura, T.; Ikeda, I. *Macromolecules* **2001**, 34, 1391. (c) Maeda, Y.; Nakamura, T.; Ikeda, I. *Macromolecules* **2001**, *34*, 8246.
(30) (a) Terada, T.; Maeda, Y.; Kitano, H. *J. Phys. Chem*. **1993**, *97*, 3619. (b) Maeda, Y.; Tsukida, N.; Kitano, H.; Terada, T.; Yamanaka, J. *J. Phys. Chem*. **1993**, *97*, 13903.
(31) Maeda, Y.; Yamamoto, H.; Ikeda, I. *Macromolecules* **2003**, *36*, 5055.
(32) Kato, E.; Murakami, T. *Polymer* **2002**, *43*, 5607.
(33) Annaka, M.; Motokawa, K.; Nakahira, T.; Kawasaki, H.; Maeda, H.; Amo, Y.; Tominaga, Y. *J. Chem. Phys*. **2000**, *113*, 5980.
(34) Appel, R.; Xu, W.; Zerda, T. W.; Hu, Z. *Macromolecules* **1998**, *31*, 5071.
(35) Suzuki, Y.; Suzuki, N.; Takasu, Y.; Nishio, I. *J. Chem. Phys*. **1997**, *107*, 5890.
(36) Kitamura, N.; Hosoda, Y.; Iwasaki, C.; Ueno, K.; Kim, H.-B. *Langmuir* **2003**, *19*, 8484.
(37) Misawa, H.; Koshioka, M.; Sasaki, K.; Kitamura, N.; Masuhara, H. *J. Appl. Phys*. **1991**, *70*, 3829.
(38) (a) Mizuno, K.; Ochi, T.; Shindo, Y. *J. Chem. Phys*. **1998**, *109*, 9502. (b) Gu, Y.; Kar, T.; Scheuner, S. *J. Am. Chem. Soc*. **1999**, *121*, 9411.
(39) Ashkin, A.; Dziedzic. J. M.; Bjorkholm, J. E.; Chu. S. *Opt. Lett*. **1986**, *11*, 288.
(40) Cherney, D. P.; Bridges, T.; Harris, J. M. *Anal. Chem*. **2004**, *76*, 4920.